

The sintering and stability of the tetragonal phase of zirconia with additions of TiO_2

V.C. Pandolfelli* and R. Stevens[†]

*Universidade Federal de S. Carlos - DEMa - C.P. 676, CEP 13560 - S. Carlos - S.P. - Brazil.

[†]University of Leeds - School of Materials - Division of Ceramics Leeds LS2 9JT - England.

ABSTRACT

The production of tetragonal zirconia polycrystalline (TZP) ceramics and identification of factors controlling the stability of the tetragonal phase in the $ZrO_2.TiO_2$ system has been investigated. In this binary system, it was not possible to retain tetragonal zirconia polycrystals at room temperature for compositions sintered above 1200°C. A decrease in the martensitic transformation temperature of zirconia was observed with titania addition, but the effect was insufficient to retain the tetragonal phase at room temperature. In solid solution, TiO_2 additions act to suppress ZrO_2 densification, this leading to grain growth when attempts are made to attain higher densities. The use of fine powders, fast firing or sintering in reducing conditions altered densification but was not able to retain a final grain size sufficiently small to avoid spontaneous tetragonal \leftrightarrow monoclinic transformation on cooling.

INTRODUCTION

Zirconia engineering ceramics have received considerable attention in recent years. At the present time, by controlling the microstructure and stabilizer content, tetragonal zirconia polycrystals (TZP) can be produced to give a variety of combinations of strength and toughness. Economics dictates the requirement for less expensive dopants to zirconia in order to stabilise the tetragonal form and for the development of optimum properties.

Although no definitive version of the $ZrO_2.TiO_2$ phase diagram is yet available, at first sight TiO_2 appears to be a good candidate considering the large tetragonal zirconia solid solution range and the low eutectoid temperature developed in this system (Fig. 1).

In the present study, zirconia ceramics in the $ZrO_2.TiO_2$ system have been investigated with the following objectives:

- a) To attempt the production of tetragonal zirconia polycrystalline ceramic using compositions and conditions hitherto not investigated.
- b) To obtain a better understanding of the factors that could lead to tetragonal zirconia stabilization.

EXPERIMENTAL PROCEDURE

Powders were prepared by coprecipitation of zirconium n-propoxide and titanium isopropoxide in a continuously stirred H_2O/NH_4OH solution retained at pH = 10. After separation from the liquid, the precipitate was washed three times with isopropyl alcohol. Following drying at 80°C, the powder was

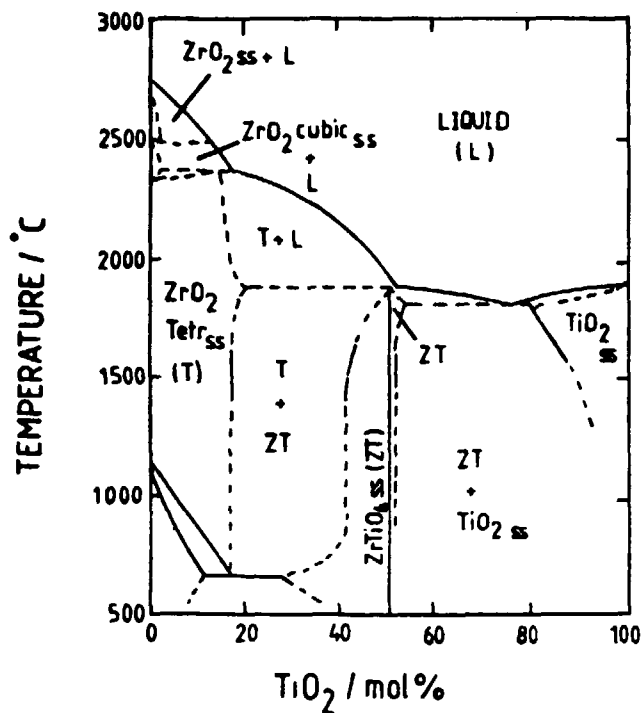


Fig. 1: Tentative phase diagram of ZrO₂.TiO₂ system⁽¹⁾.

calcined at 950°C for 30 min. and subsequently micronized in alcohol using zirconia cylinders. The calcination programme was based on the results of thermogravimetric and differential thermal analysis.

X-ray fluorescence (XRF) spectrometry was used to analyse the composition of all calcined powders in the ZrO₂.TiO₂ system. To provide reproducible and accurate analyses, the fusion technique was used to prepare samples of standards and unknown compositions. Fusion helps to overcome problems arising from particle size, surface state and absorption effects.

The sintering behaviour of green compacts under isothermal conditions in air and reducing atmospheres was investigated using a sinter dilatometer. Assuming isotropic shrinkage during sintering, a computer programme converted the LVDT voltage reading into specimen density. Using curve fitting routines, the densification rates which occur at different times were obtained. For the reducing conditions, a mixture of 8 vpm of carbon dioxide in 5.01 vol.% carbon monoxide balanced with argon was used as the sintering atmosphere.

Phase analysis and lattice parameter determination of the calcined powders and sintered discs were performed using an X-ray diffractometer with Ni-filtered Cu radiation. The volume fraction of the monoclinic and tetragonal phases present were calculated using Toraya's equation⁽²⁾ assuming the constant $P = 1.31$.

A standard multi-point gas adsorption technique was used to evaluate the surface area of the powders prior to and the pellets after sintering.

RESULTS

A range of compositions in the $ZrO_2.TiO_2$ system was prepared by altering the amount of TiO_2 present. An average of 0.8 mol.% of hafnium was detected in the zirconia produced by coprecipitation of the alkoxides. The similar chemical properties of ZrO_2 and HfO_2 allow the latter to be considered as part of zirconia for compositional calculations.

Quantitative phase analyses, lattice volume and the ratio between the (004) and (400) lattice parameters for the $ZrO_2.TiO_2$ powders calcined at 950°C are shown in Table 1. Phases other than monoclinic or tetragonal solid solutions of zirconia were not found in the calcined powders.

Table 1: Quantitative phase analysis, lattice volume and tetragonal lattice parameter ratio (c/a) for the $ZrO_2.TiO_2$ powders calcined at 950°C.

Composition (mol.%)	Tetragonal volume fraction (%)	Vol. (nm ³)	c/a
92.37 ZrO_2 -7.63 TiO_2	25.3 ± 0.2	0.13362	1.0236 ± 0.0005
88.47 ZrO_2 -11.53 TiO_2	70.4 ± 1.6	0.13360	1.0250 ± 0.0003
85.21 ZrO_2 -14.78 TiO_2	94.0 ± 0.6	0.13324	1.0265 ± 0.0001
82.11 ZrO_2 -17.89 TiO_2	100	0.13305	1.0294 ± 0.0004
78.47 ZrO_2 -21.53 TiO_2	100	0.13295	1.0317 ± 0.0001

For sintering experiments, the calcined powders were die pressed at 190 MPa. Using heating and cooling rates of 300°C/hr, pellets were sintered at 1350°C, 1450°C and 1550°C for 2 hours. Results for the green and final sintered density are given in Table 2.

Table 2: Green and final density of $ZrO_2.TiO_2$ compositions sintered at different temperatures.

Composition (mol.%)	Dwell time at 1200°C (min)			
	10	30	60	90
ZrO_2	59.1 ± 3.0	65.7 ± 4.2	70.8 ± 1.3	72.7 ± 1.9
92.37 ZrO_2 -7.63 TiO_2	55.0 ± 1.4	57.4 ± 1.1	59.6 ± 0.8	60.5 ± 1.0
88.47 ZrO_2 -11.53 TiO_2	49.8 ± 0.5	52.2 ± 0.5	52.6 ± 0.3	52.8 ± 0.5
85.21 ZrO_2 -14.78 TiO_2	46.3 ± 0.3	47.3 ± 0.6	47.5 ± 0.4	47.3 ± 0.7
82.11 ZrO_2 -17.89 TiO_2	43.3 ± 0.4	43.6 ± 0.5	44.2 ± 0.2	44.1 ± 0.5
78.47 ZrO_2 -21.53 TiO_2	40.5 ± 0.2	41.0 ± 0.2	40.9 ± 0.2	41.2 ± 0.5

After sintering, none of the tetragonal phase had been retained in any of the compositions. With the exception of the composition without TiO_2 and that with 21.53 mol.% TiO_2 , all the samples sintered at 1550°C were found to have fallen apart as a consequence of the martensitic $t \rightarrow m$ transformation during cooling. The presence of $ZrTiO_4$ has been confirmed only in the compositions with 17.89 mol.% and 21.53 mol.% TiO_2 . Comparative results were obtained by Bateman⁽³⁾ studying the ZrO_2 .15 mol.% TiO_2 composition.

Using a sinter dilatometer with controlled atmosphere, the changes of density with time and the densification rate with density were obtained. Figure 2 shows the effect of TiO_2 addition on the densification rate of zirconia sintered in air at 1200°C. Only the monoclinic zirconia phase was detected for all the compositions when sintering took place at 1200°C. Results in Fig. 2 clearly indicate that when in solid solution, the TiO_2 addition is inhibiting the densification of zirconia.

The influence of air and reducing atmosphere on the sinterability of ZrO_2 and the 78.47 ZrO_2 -21.53 TiO_2 mol.% composition is presented in Figure 3. The oxygen partial pressure p_2 was calculated using Turkdogan tables⁽⁴⁾ as 2.4×10^{-19} atm at 1200°C and 1.84×10^{-16} atm at 1450°C. Tetragonal zirconia was not retained in any of the compositions sintered under reducing conditions.

To study the influence of TiO_2 on the transformation temperature of zirconia, measurements have been carried out to determine the temperature range for the martensitic transformation. Table 3 shows the start and finish of the tetragonal \leftrightarrow monoclinic transformation during cooling (M_s and M_f temperature respectively) and on heating (A_s and A_f). No further changes in the transformation temperature were observed when compositions in the ZrO_2 . TiO_2 system were sintered in reducing atmospheres.

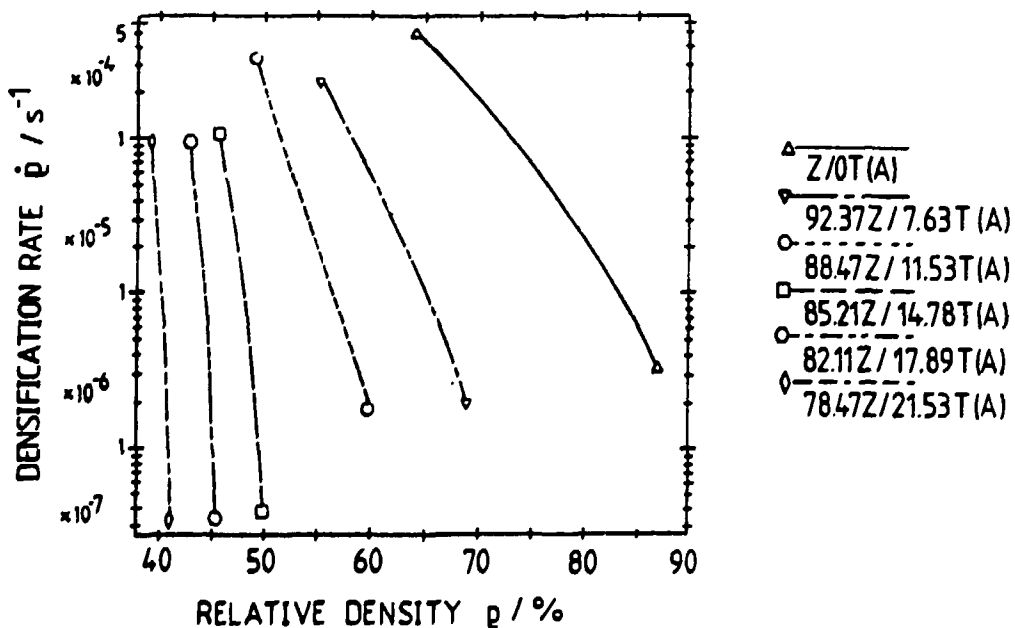


Figure 2: Densification rate versus relative density for ZrO_2 . TiO_2 compositions sintered in air (A) at 1200°C. Each curve represents the best fit for a range of 50 data points. [Z = ZrO_2 , T = TiO_2]

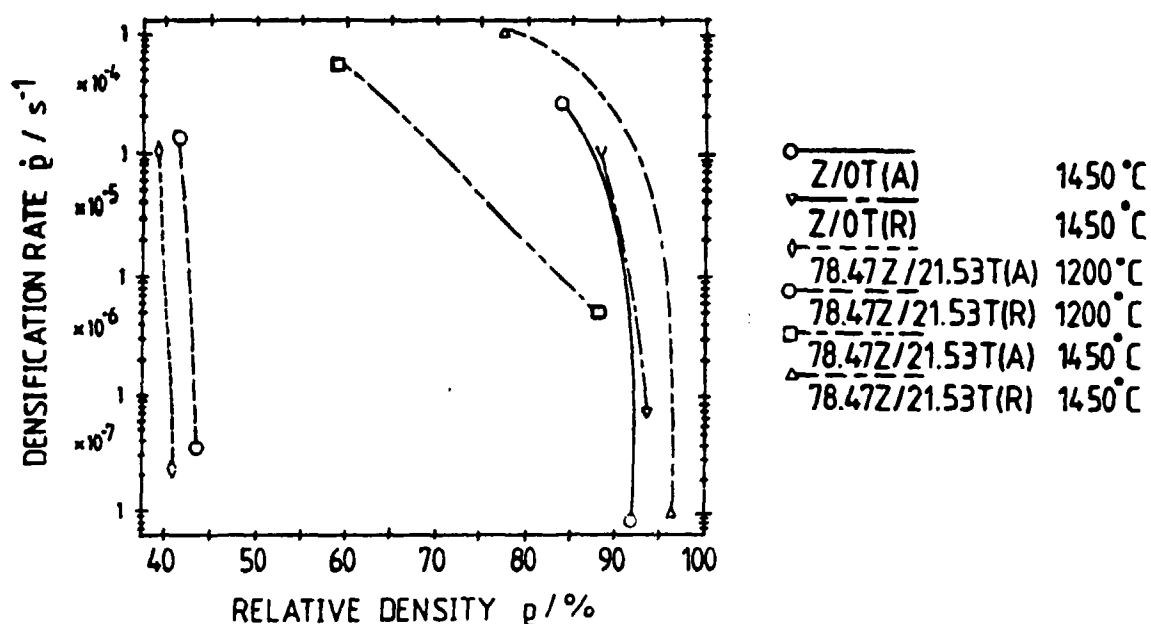


Figure 3: Densification rate versus relative density for ZrO_2 and $78.47 ZrO_2-21.53 TiO_2$ mol.% composition sintered in air (A) and reducing atmosphere (R).

Table 3: Influence of TiO_2 on the martensitic transformation temperature of ZrO_2 .

Composition (mol.%)	M_s (°C)	M_F (°C)	A_s (°C)	A_F (°C)
ZrO_2	925	830	1090	1160
92.37 $ZrO_2-7.63 TiO_2$	775	730	990	1060
88.47 $ZrO_2-11.53 TiO_2$	692	656	840	910
85.21 $ZrO_2-14.78 TiO_2$	559	537	750	820
82.11 $ZrO_2-17.89 TiO_2$	431	410	570	700
78.47 $ZrO_2-21.53 TiO_2$	326	220	454	640

Since the driving force for both the densification and coarsening processes is related to the reduction in surface area, Burke et al. (5) suggested that materials with different coarsening and densification behaviour should be distinguished by the different shape of their surface area reduction trajectories. Considering a graph where surface area is plotted against relative density, in the case of pure coarsening, the surface area will be reduced with no increase in density, as shown by trajectory A in Fig. 4. When the reduction of the surface area is occurring wholly by mechanisms that

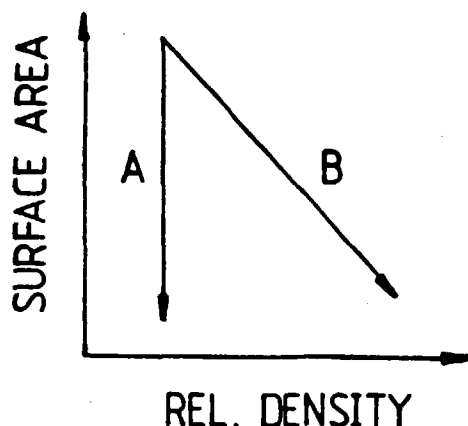


Figure 4: Surface area and relative density relationship during sintering. A is the trajectory for pure coarsening and B for pure densification.

result in densification, then trajectory B is obtained. The more typical sintering behaviour of real compacts is described by a series of curves between the two extremes, due to simultaneous contributions of both mechanisms.

In order to obtain further information concerning the influence of TiO_2 on the sinterability of ZrO_2 , the model of Burke et al.⁽⁵⁾ was applied to the $ZrO_2.TiO_2$ system. The results for $ZrO_2.TiO_2$ compositions sintered for different times at 1200°C, shown in Figure 5, represent an average of at least three measurements for each sample.

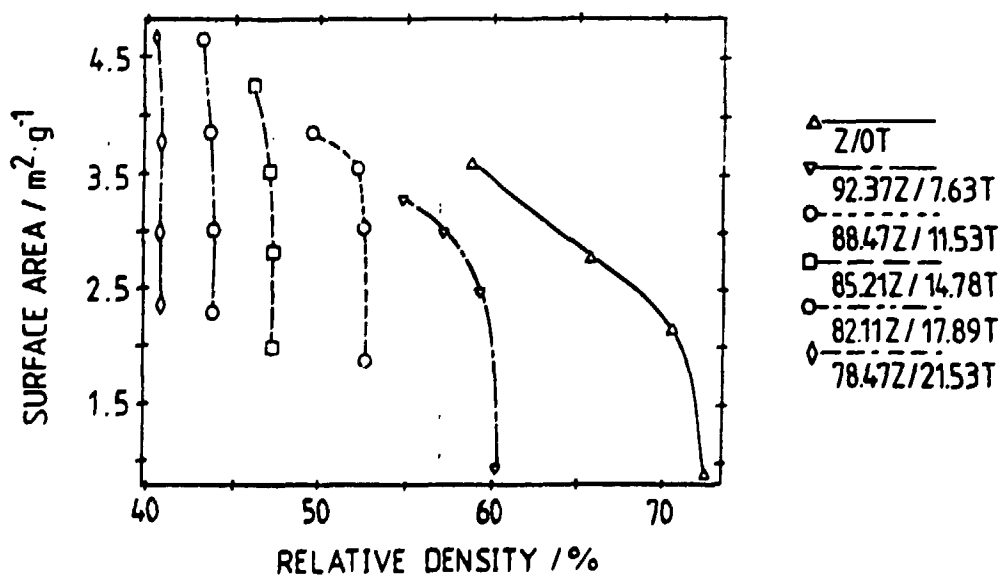


Figure 5: Surface area versus relative density for pellets of $ZrO_2.TiO_2$ compositions sintered for different times at 1200°C.

Improvements in densification with a reduction of grain growth can be obtained by fast firing⁽⁶⁾. The effectiveness of this process can be understood in terms of the difference of the activation enthalpies for the densification and coarsening mechanisms⁽⁷⁾. In materials where the enthalpies for lattice and boundary diffusion are higher than for surface diffusion, the higher the sintering temperature, the larger will be the densification/coarsening ratio. Data for activation enthalpies of the relevant diffusion coefficients are not at present available and therefore the best way to assess the operating mechanisms is by experiment.

Fast firing experiments were carried out in a tube furnace at temperatures of 1400°C, 1500°C and 1600°C. The pellets, laid on a highly porous alumina base, were automatically pushed into the hot zone of the furnace taking ~120 seconds to reach the maximum temperature. After a dwell time of 15 minutes they were moved to a region of the furnace at 200°C. All the experiments were repeated using commercial tetragonal zirconia (TS-12 Ce and TS-3Y) and pure commercial zirconia (Dynazirkon (R)F) to establish whether thermal shock damage would affect interpretation of the results. Compositions containing titania resulted in complete disintegration after fast firing for 15 minutes at 1400°C, 1500°C and 1600°C. Table 4 shows the fast firing results at 1600°C.

Table 4: Final density of zirconia pellets after fast firing at 1600°C for 15 minutes.

Composition	Final Density (g/cm ³)
Dynazirkon (R)F	5.05 ± 0.01
TS-12Ce (12 mol.% CeO ₂)	5.64 ± 0.02
TS-3Y (3 mol.% Y ₂ O ₃)	5.89 ± 0.01
ZrO ₂	5.41 ± 0.07
All compositions in the ZrO ₂ .TiO ₂ system	Disintegration

To verify whether any remnant product of the calcination in the powders prepared by the alkoxide route could cause the differences in densification behaviour found amongst the ZrO₂.TiO₂ compositions, infrared spectrographic analysis was performed. The powders, 0 mol.%, 14.78 mol.% and 21.53 mol.% of TiO₂, were calcined at 850°C, 1100°C and 1300°C. A heating rate of 300°C/hour and a dwell time of 1 hour at the maximum temperature was used for all the calcinations. The samples for infrared analysis were prepared by careful mixing and vacuum pressing of 3 mg of calcined powders with 300 mg of KBr. The transmission infrared spectra of the calcined powders were determined in the range 4000 to 500 cm⁻¹.

Results show that all three powders calcined at 850°C have bands which can be assigned to C-H and O-H bond stretching respectively. Their presence is associated with residues from the alkoxides reaction. After calcination at higher temperatures, oxidation of the residues is complete and the bands are no longer present. The presence of monoclinic zirconia is verified by bands at 740 cm⁻¹ and 515 cm⁻¹ in the spectrum of zirconia calcined at 850°C. The intensity of this band is greatly reduced in the powder with 14.78 mol.% of

TiO₂ calcined at this temperature and is not apparent in the spectrum of the composition with 21.53 mol.% TiO₂. On calcination at higher temperatures the intensity of the monoclinic absorption band increases for all three compositions in agreement with the XRD results.

In a final experiment to ascertain the influence of the nature of the powder on the sinterability of zirconia-titania compositions, commercial zirconia (Dynazirkon (R)F) and commercial rutile (TiO₂) were wet ball milled in the same proportions as for the powders prepared by the alkoxide route. The mixed powders were then calcined at 950°C and were found not to show any tetragonal stabilization. The presence of a strong rutile peak in the XRD trace inferred that the extent of solid solution was limited. For the mixed oxide powders, the final densities of pellets sintered at 1200°C and 1350°C for 2 hours did not show a large decrease in relative density as the TiO₂ is incorporated to zirconia. However, XRD shows that complete solid solution has not taken place, suggesting that TiO₂ agglomerates had sintered before further solid solution formation. Tetragonal zirconia was not detected in any of the experiments involving mixtures of the commercial powders. Results obtained from the mixed powders experiments have demonstrated the need to use the alkoxide route to produce powders to study the effect of TiO₂ on the sintering and stabilization of ZrO₂.

DISCUSSION

In the ZrO₂-TiO₂ system, when sintering took place above 1200°C, the t ↔ m transformation was not suppressed sufficiently to retain tetragonal zirconia at room temperature.

The reasons for retention of metastable tetragonal zirconia at room temperature are still the subject of considerable discussion. Considering the same grain morphology and absence of glassy phase at the grain boundary, factors that could be of importance on tetragonal stabilization include: the oxygen ion vacancy content, the cationic radius and the crystal structure of the dopant oxide, the chemical free energy of the t ↔ m transformation and the critical grain size for spontaneous transformation.

The factors that influence stabilization may well be interconnected; however discussion of how each variable might individually affect the ZrO₂-TiO₂ system will help to identify which is of greatest significance.

It is known that oxygen vacancies created either by reducing the oxygen partial pressure or by alloying zirconia with aliovalent metal oxides (Mg²⁺, Ca²⁺ and Y³⁺) play an important role in stabilizing the cubic structure⁽⁸⁻¹⁰⁾. Cubic stabilization can be considered as the thermodynamic response of the system to the need for accommodation of a large number of anion vacancies produced during sintering⁽¹¹⁾. Although a decrease of the cubic-tetragonal transformation temperature for low pO₂ is shown in the Zr-O phase diagram⁽⁸⁾, previous researchers have indicated that the tetragonal to monoclinic transformation remains unaffected by pO₂^(12,13).

It can be seen in Figure 3 that defects generated by TiO₂, either (i) by increasing the temperature or (ii) sintering in reducing conditions, are important in increasing the ZrO₂-TiO₂ sinterability. However, the presence of such defects did not manifest itself in any positive effect on the retention of tetragonal zirconia at room temperature.

Considering the ZrO₂-CeO₂ system fully tetragonal zirconia is obtained when a composition with 12 mol.% of ceria is sintered in air, providing the

final grain size remains below 3-4 μm . It is known that above 685°C, CeO_2 may exhibit large deviations from stoichiometry, which may extend to a maximum at $\text{CeO}_{1.78}$ at and above 1023°C⁽¹⁴⁾. Experiments undertaken as part of this study show that sintering Ce-tetragonal zirconia in a reducing atmosphere gives monoclinic zirconia plus $\text{Ce}_2\text{Zr}_2\text{O}_7$ ⁽¹⁵⁾. Therefore if the presence of oxygen vacancies is important for the tetragonal stabilization in the $\text{ZrO}_2\text{-CeO}$ system, perhaps the concentration of oxygen vacancies should be limited such that the CeO_{2-x} could remain in solid solution (Fig. 6), avoiding formation of the second phase.

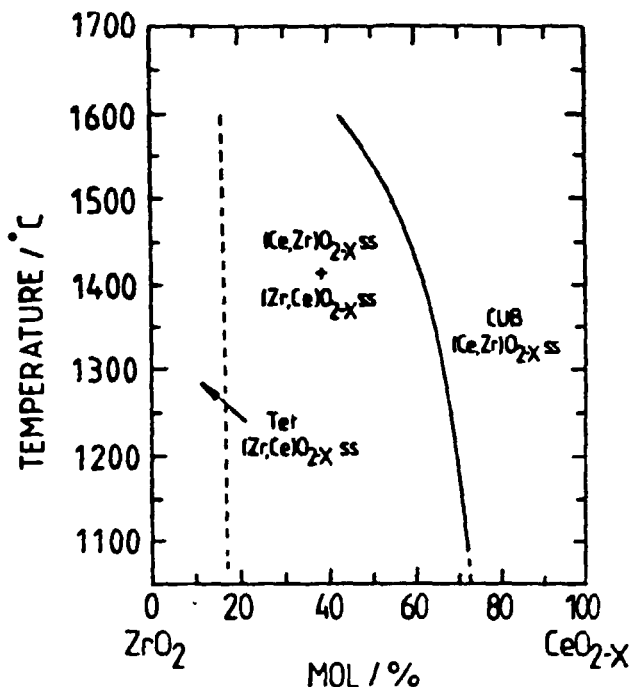


Figure 6: System $\text{ZrO}_2\text{-CeO}_{2-x}$ in air in the 1100°C to 1600°C temperature range⁽¹⁶⁾.

Thus although the influence of oxygen vacancies in cubic zirconia stabilization can be ascertained, in general their importance for the retention of tetragonal zirconia at room temperature is not clear in relation to the $\text{ZrO}_2\text{-TiO}_2$ and $\text{ZrO}_2\text{-CeO}_2$ systems.

The cationic radius and the crystal symmetry of the dopant are further important parameters contributing to zirconia stabilization. Titanium ($\text{Ti}^{4+} = 0.74 \text{ \AA}$)⁽¹⁷⁾ has a smaller cationic radius than zirconium ($\text{Zr}^{4+} = 0.84 \text{ \AA}$) and tetragonal zirconia polycrystalline ceramics (TZP) have not been produced using this ion. On the other hand cations such as magnesium ($\text{Mg}^{2+} = 0.89 \text{ \AA}$), cerium ($\text{Ce}^{4+} = 0.97 \text{ \AA}$), yttrium ($\text{Y}^{3+} = 1.019 \text{ \AA}$) and calcium ($\text{Ca}^{2+} = 1.12 \text{ \AA}$), in which the ionic radius is larger than the Zr^{4+} , have all been used to stabilize zirconia ceramics. Based on the crystal structure of the dopants mentioned above, it appears that only solute oxides having a cubic structure are able to stabilize the cubic and/or the tetragonal phase in zirconia. MgO and CaO both have a cubic NaCl structure, CeO_2 has a cubic fluorite structure, Y_2O_3 a cubic bixbyite structure, whereas TiO_2 has a tetragonal rutile structure⁽¹⁸⁾. Although results related to the cationic radius and crystal symmetry of the most common dopants (MgO, CaO, Y_2O_3 and CeO_2) could indicate that those having ions larger than zirconia and forming oxides with

cubic structure would be more likely to produce TZP ceramics, this trend cannot be generalized. Dopants such as Nd_2O_3 , Yb_2O_3 , Gd_2O_3 , Eu_2O_3 and La_2O_3 all have the same crystal structure as Y_2O_3 and a cationic radius larger than zirconia, but so far fully tetragonal zirconia polycrystals have not yet been produced using these oxides(19,20).

A consistent factor pertaining to tetragonal zirconia retention is the critical grain size for spontaneous $t \leftrightarrow m$ transformation. Considering Heuer's(21) and Chen's(22) approach, the critical grain size at a given temperature can be defined as the size below which the probability of each grain containing a critical nucleus is less than unity. Typically it is less than $3 \mu\text{m}$ for the CeO_2 -TZP and is in the range 0.5 - $1.0 \mu\text{m}$ for Y_2O_3 -TZP.

Table 3 and the phase diagram of the ZrO_2 - TiO_2 system (Fig. 1) show that TiO_2 additions reduce the chemical free energy for the tetragonal to monoclinic phase transformation but give no indication of how TiO_2 might affect the final grain size of zirconia. Applying Burke's model to the ZrO_2 - TiO_2 system (Fig.5), shows that on addition of titania, the densification component is gradually reduced until almost pure coarsening occurs for the 78.47 ZrO_2 -21.53 TiO_2 mol.% composition. These results were confirmed by grain size measurements on the polished surfaces of the 21.53 mol.% TiO_2 composition ceramics.

For systems which do not densify significantly, vapour transport and surface diffusion have been suggested as the predominant mass transport mechanisms. Vapour transport occurs by an evaporation-condensation process and the extent to which it occurs depends on the vapour pressure of the material being sintered. For most oxides in use as engineering ceramics, vapour phase transport is usually only of importance at very high temperatures, close to the melting point. In the ZrO_2 - TiO_2 system, owing to the low volatility of zirconium and titanium oxide (23), it is to be expected that surface diffusion would play a major role in the coarsening process at low temperature. Titania might act to inhibit sintering in zirconia by increasing the surface diffusion coefficient in the material and hence increasing the coarsening rate. Other researchers agree that TiO_2 additions accelerate grain growth and act to suppress densification in Y_2O_3 -TZP ceramics(24,25). Osendi et al.(26) showed that although TiO_2 increases the initial sintering rate of the Al_2O_3 -8 vol.% ZrO_2 composites, a significant enhancement of the grain growth kinetics of ZrO_2 was observed after annealing.

In order to avoid coarsening and promote sintering, three principal procedures can be utilised.

a) Fine, homogeneous powder.

In the present study, the use of a fine, chemically homogeneous powder produced by the alkoxide route was found not to give a dense ceramic after sintering. The decrease of sinterability with TiO_2 additions to ZrO_2 cannot be associated with the powder preparation route, since surface area results, agglomerate strength, electron microscopy and infrared analysis showed no significant property differences among the powders.

b) Fast Firing.

Fast firing was ineffective in generating the small grain size required to retain the tetragonal phase. Measurements of final density after fast firing ZrO_2 - TiO_2 compositions was not possible; however the final grain size was obviously above the critical size since the martensitic transformation could not be avoided.

c) Hot pressing.

Hot pressing experiments undertaken using graphite punches and a graphite die led to reduction of the zirconium oxide and to the formation of titanium carbide. The use of an alumina punch and die set was considered, but rejected due to the chemical reactions which could occur between the sample and the alumina die.

CONCLUSIONS

- 1) In the $ZrO_2.TiO_2$ system, tetragonal zirconia polycrystals have not been retained at room temperature for compositions sintered above 1200°C. Despite the decrease of the martensitic transformation temperature of zirconia with titania additions, this was in itself insufficient to retain the tetragonal phase at room temperature.
- 2) The lattice defects generated by sintering $ZrO_2.TiO_2$ compositions in reducing atmosphere have improved densification but did not show any positive effect on retention of the tetragonal zirconia at room temperature. Studies carried out in the $ZrO_2.TiO_2$ system, $ZrO_2.CeO_2$ system and an analysis of results available in the literature, show that the influence of oxygen vacancies, cationic radius and crystal structure of dopant on stabilization of tetragonal zirconia is yet to be clearly explained.
- 3) In solid solution TiO_2 additions act to suppress the ZrO_2 densification, leading to grain growth when attempts are made to attain higher densities. This is believed to be the main factor preventing retention of tetragonal zirconia at room temperature in the $ZrO_2.TiO_2$ system. The use of fine powders and fast firing techniques was not able to keep the final grain size small enough to avoid spontaneous $t \leftrightarrow m$ transformation on cooling.

ACKNOWLEDGEMENTS

V.C. Pandolfelli would like to thank CNPq process no. 20.2522/84 for sponsoring his studies at Leeds University. The helpful discussions with Professor R.J. Brook and Dr. I. Nettleship were also greatly appreciated.

REFERENCES

1. NOGUCHI, T. and MIZUMO, M. Bull. Chem. Soc. Jap. 41 (1968) 2895.
2. STEVENS, R. Introduction to Zirconia, M.E.L., U.K., 1986.
3. BATEMAN, C.A. Master Sc. Diss., Lehigh Univ., U.S.A., 1986.
4. TURKDOGAN, E.T. Physical Chemistry of High Temperature Technology. Academic Press, U.S.A., 1980.
5. BURKE, J.E., et al. Mat. Sci. Res. 13 (1979) 417.
6. WU, S. Ph.D. Thesis, Leeds University, U.K., 1982.
7. MOSTAGHACI, H. and BROOK, R.J. Trans. J. Br. Ceram. Soc. 82 (1983) 167.
8. RUH, R. and GARRET, H.J. J. Am. Ceram. Soc. 50 (1967) 257.
9. HEUER, A.H. and RÜHLE, M. In Advances in Ceramics Vol. 12, Science and Technology of Zirconia 2, edited by Claussen, N., Rühle, M. and Heuer, A.H., The Am. Ceram. Soc., U.S.A., p.1, 1983.
10. HO, S.M. Mat. Sci. and Eng. 54 (1982) 23.
11. RAMASWAMY, P. and AGRAWAL, D.C. J. Mat. Sci. 22 (1987) 1243.
12. CARNIGLIA, S.C. et al. J. Am. Ceram. Soc. 54 (1971) 13.
13. RAUH, E.G. and GARG, S.P. J. Am. Ceram. Soc. 63 (1980) 239.
14. KOFSTAD, P. Nonstoichiometry, diffusion and electrical conductivity in binary metal oxides. Wiley-Interscience, U.S.A., 1972.

15. PANDOLFELLI, V.C. Unpublished results, Leeds Univ., U.K., 1988.
16. ROTH, S.R. et al. Phase Diagrams for Ceramists Vol. 6, The Am. Ceram. Soc., U.S.A., 1987.
17. SHANNON, R.D. Acta Cryst. A32 (1976) 751.
18. WYCKOFF, R.W.G. Crystal Structure Vol. 1 and 2, Interscience Publ., U.K., 1964.
19. KÖHLER, E.K. and GLUSHKOVA, V.B. In Science of Ceramics 4, edited by Stewart, G.H., Brit. Cer. Soc., U.K., p.233, 1968.
20. BASTIDE, B. et al. J. Am. Ceram. Soc. 71 (1988) 449.
21. HEUER, A.H. and RÜHLE, M. Acta Metall. 33 (1985) 2101.
22. CHEN, I.W. and CHIAO, Y.H., p.33 in Ref. 9.
23. CHANDRASEKHARAI AH, M.S., in The Characterization of High Temperature Vapours. Edited by Morgrave, J.L. Wiley-Interscience, U.S.A., p.495, 1967.
24. TSUKUMA, J. J. Mat. Sci. Lett. 5 (1986) 1143.
25. SATO, T. et al. Int. J. High Tech. Cer. 2 (1986) 167.
26. OSENDI, M.I. and MOYA, J.S. J. Mat. Sci. Lett. 7 (1988) 15.
27. ALDEBERT, P. and TRAVERSE, J.P. J. Am. Ceram. Soc. 68 (1985) 34.
28. WU, S. and BROOK, R.J. J. Br. Ceram. Soc. 82 (1983) 200.

APPENDIX

Zirconia Sintering in Reducing Conditions

For zirconia pellets with the same initial green density, Fig. 3 shows that sintering in reducing atmosphere yielded a slightly higher densification rate than pellets sintered in air. Assuming that (i) sintering at low pO_2 increases the concentration of oxygen vacancies, and (ii) the rate controlling species for densification in zirconia is cationic⁽¹⁰⁾, since the diffusion coefficients of cations in zirconia are several orders of magnitude less than the values for oxygen (Table 5); the results of Fig. 3 can only be explained if the concentration of cationic defects increases at a greater rate than the oxygen vacancy concentration.

Table A1: Diffusion coefficients of oxygen and zirconium in pure zirconia (27).

Temperature (°C)	log D (cm ² .s ⁻¹)	
	oxygen	zirconium
1100	-12	-17
1300	-6	-14
1900	-	-11

In order to examine further this possibility the defect chemistry of zirconia needs to be analyzed.

At low pO_2 the concentration of oxygen vacancies [$V_O^{\bullet\bullet}$] is assumed to be greater than the concentration of zirconium vacancies [V_{Zr}''], oxygen interstitials [O_i''], electron holes (p)* and zirconium interstitials, [$Zr_i^{\bullet\bullet}$].

*In the case of electrons and positive holes the concentration of these defects are often written as n and p, instead of [e'] and [h'] respectively.

Thus the following electroneutrality condition can be used:

$$2[V_0^{\bullet\bullet}] = n \quad (A1)$$

Applying the mass-action relationship for the defect equilibria equations below:

$$O^x = V_0^{\bullet\bullet} + 2e' + \frac{1}{2} O_2 \text{ (for low } pO_2) \quad (A2)$$

$$n_i = V_{Zr}^{\bullet\bullet\bullet} + 2V_0^{\bullet\bullet} \quad (A3)$$

$$n_i = e' + h' \quad (A4)$$

$$O_0^x = V_0^{\bullet\bullet} + O_i^{\bullet} \quad (A5)$$

$$Zr_{Zr}^x = V_{Zr}^{\bullet\bullet\bullet} + Zr_i^{\bullet\bullet\bullet\bullet} \quad (A6)$$

and using the neutrality condition (eq. A1), the following trends for the concentration of defects with the oxygen partial pressure are obtained:

$$[V_0^{\bullet\bullet}] \propto [O_2]^{-1/6} \quad (A7)$$

$$[Zr_i^{\bullet\bullet\bullet\bullet}] \propto [O_2]^{-1/3} \quad (A8)$$

$$[O_i^{\bullet}] \propto [O_2]^{1/6} \quad (A9)$$

$$[V_{Zr}^{\bullet\bullet\bullet}] \propto [O_2]^{1/3} \quad (A10)$$

$$n \propto [O_2]^{-1/6} \quad (A11)$$

$$p \propto [O_2]^{1/6} \quad (A12)$$

As seen from the equations A7 and A8, both $[V_0^{\bullet\bullet}]$ and $[Zr_i^{\bullet\bullet\bullet\bullet}]$ increase at significantly different rates as the oxygen partial pressure is reduced in the range where the neutrality condition is valid (Fig. A1).

Under such conditions, the increased rate of $[Zr_i^{\bullet\bullet\bullet\bullet}]$ formation compared to $[V_0^{\bullet\bullet}]$ could explain the higher densification rate shown by the zirconia pellets sintered in reducing atmosphere. These results agree with those obtained by Wu⁽²⁸⁾ sintering zirconia in air with different amounts of CaO.

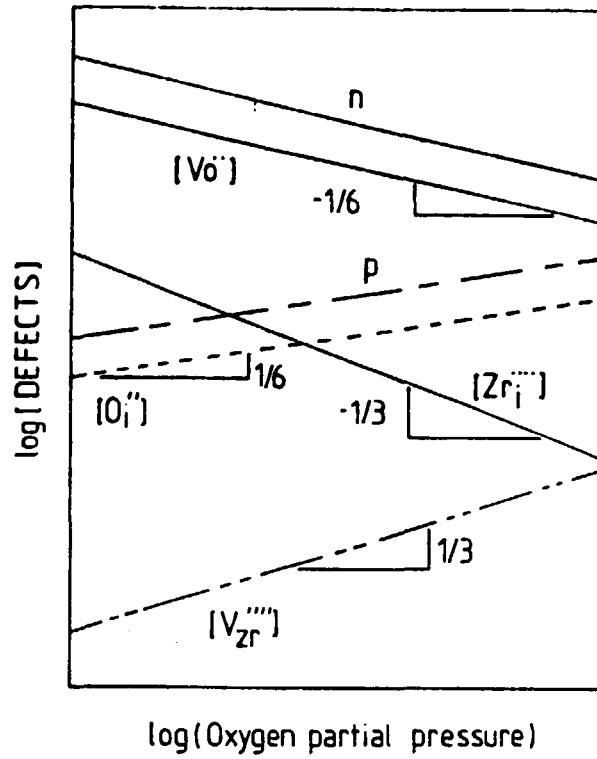


Figure A1: Brouwer diagram showing the variation of defect concentrations with oxygen partial pressure in pure zirconia. Neutrality condition assumed $n = 2[\text{V}_\text{O}^{\bullet\bullet}]$.